THE JOURNAL OF PHYSICAL CHEMISTRY C

Article

pubs.acs.org/JPCC

Hindered Translator and Hindered Rotor Models for Adsorbates: Partition Functions and Entropies

Lynza H. Sprowl,[†] Charles T. Campbell,[‡] and Líney Árnadóttir*[,†]

[†]School of Chemical, Biological and Environmental Engineering, Oregon State University, Corvallis, Oregon 97331-2702, United States

[‡]Department of Chemistry, University of Washington, Seattle, Washington 98195-1700, United States

Supporting Information

ABSTRACT: With the recent explosion in computational catalysis and related microkinetic modeling, the need for a fast yet accurate way to predict equilibrium and rate constants for surface reactions has become more important. Here we present a fast and accurate new method to estimate the partition functions and entropies of adsorbates based on quantum mechanical estimates of the potential energy surface. As with previous approaches, it uses the harmonic oscillator (HO) approximation for most of the modes of motion of the adsorbate. However, it uses hindered translator and hindered rotor models for the three adsorbate modes associated with motions parallel to the surface and evaluates these using an approach based on a method that has proven accurate in modeling the internal hindered rotations of gas molecules. The adsorbate entropies were calculated with this method for four adsorbates (methanol, propane, ethane, and methane) on Pt(111) using density functional theory (DFT) to evaluate the potential energy surface and are shown to be in very good agreement with experiments, better than using only the HO approximation. The translational and rotational contributions to the entropy of a hindered translator/hindered rotor are very closely approximated by the corresponding harmonic oscillator entropy (within 0.46 R) when the barrier exceeds kT and by the entropy of an ideal 2D monatomic gas of the same mass and a free 1D rotor with the same moment of inertia, respectively (within 0.12 R), when the barrier is less than kT. However, the harmonic oscillator/lattice gas model severely overestimates the entropy when kT exceeds the barrier.

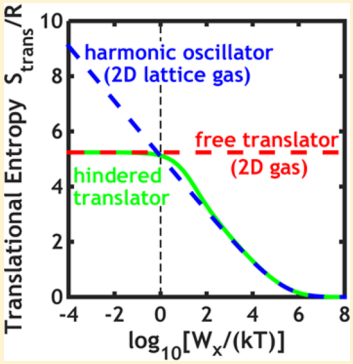

1. INTRODUCTION

Adsorbed species on solid surfaces are involved in many reactions of great technological importance, especially in catalysis, electrocatalysis, separations, and fabrication of devices that require film growth (e.g., microelectronics and photovoltaics). As such, there has been tremendous effort worldwide to learn how to predict reaction rates and equilibrium constants for elementary reactions involving adsorbates. Theoretical calculations of rate constants and equilibrium constants for such reactions require knowing both the enthalpy and entropy of the adsorbed species and transition states. While much effort has been devoted to measuring and calculating the enthalpies of well-defined adsorbates,[1,2] few measurements of the entropies of adsorbates have been reported until Campbell and Sellers' 2012 paper[3] where they determined the entropies of a large number of adsorbed molecules. They combined those results with many previously measured entropies to show that the standard-state entropies of adsorbed molecules are generally ~2/3 of that for the same molecule in the gas phase at 1 bar and the same temperature.[3] They noted that these entropies are larger than most theoretical predictions, which assume a lattice-gas model and use the harmonic oscillator approximation to estimate partition functions.[3] They attributed this difference to a failure of that approximation, which we explore in detail here.

Here, we derive a new theoretical method to estimate partition functions and entropies of adsorbed species based on the hindered translator and hindered rotor potential energy surfaces for motions parallel to the surface. We use this method, together with potential energy surfaces estimated from density functional theory (DFT), to compute the entropies of some typical adsorbate systems. We show that this approach is more accurate than the harmonic-oscillator ideal lattice gas approximation yet still quite easy to implement. We show that the difference between these models arises for several reasons but, surprisingly, not mainly due to a failure of the harmonic-oscillator approximation per se. Indeed, the new model (which gets the frequencies for vibrations parallel to the surface in a different way than the usual DFT calculations) gives a translational contribution to the hindered translator entropy that equals (within 0.46 R) the entropy of the 2D harmonic oscillator (i.e., ideal lattice gas) model when kT is less than the diffusion barrier and that equals (within 0.12 R) the translational entropy for an ideal 2D monatomic gas when kT exceeds that barrier (where the lattice gas approximation severely overestimates the entropy). The cutoff between these

Received: November 27, 2015
Revised: March 26, 2016
Published: March 28, 2016

DOI: 10.1021/acs.jpcc.5b11616
J. Phys. Chem. C 2016, 120, 9719−9731

two behaviors is surprisingly sharp, so that adsorbates can be treated with one simple model or the other across the whole temperature range. A similar result is found for hindered rotations. This new model (and these very simple but accurate approximations to it) should be useful to future researchers in surface chemistry since it provides more accurate predictions of standard-state entropies and partition functions and thus more accurate equilibrium constants and rate constants for surface reactions than provided by the standard harmonic oscillator approximation.

Previously, surface chemists had usually thought of adsorbate entropies in terms of the two limiting cases that have been discussed in statistical thermodynamics texts: the 2D lattice gas model and the 2D ideal gas model.[4] In calculating rate constants for surface reactions based on quantum mechanical calculations of adsorbed reactant and transition state energies (mainly by density functional theory, DFT), surface chemists almost exclusively rely on harmonic transition state theory approaches, which assume that each adsorbate is a localized oscillator with only vibrational modes.[5−10] In analyzing experimental measurements of adsorbate entropies, it was postulated that this approach underestimates the experimental entropies because adsorbates have translations and rotations parallel to the surface which are more labile. The new method presented here accurately considers the nature of the potential energy surface for these motions, which have small but significant barriers to motion parallel to the surface, with translational barriers repeating every lattice constant (or a simple constant times it) and rotational barrier periodicity determined by the surface symmetry, as shown for example in Figure 1. In principle, one must solve the Schrödinger equation

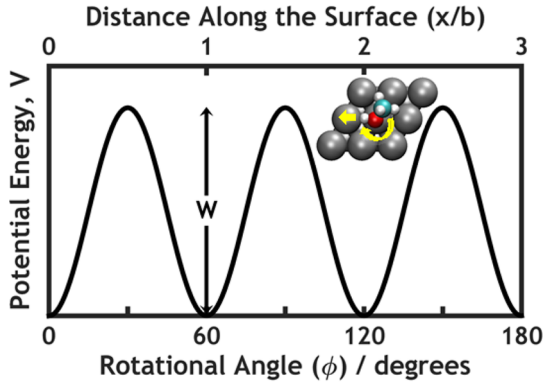

Figure 1. Example potential energy surface for adsorbate motions parallel to the surface: translation (top axis), where b is the nearest-neighbor distance between surface atoms, and rotation (bottom axis) for a surface with 3-fold symmetry.

for this potential's quantum-mechanically allowed energy levels and then sum over these states to get the partition function, q.

To simplify this, we utilized an approximation similar to that originally developed by Pitzer and Gwinn[11] for estimating partition functions of hindered internal rotations within gas molecules and later improved by Goddard's group and proven to give high accuracy.[12] To our knowledge, neither of these approximations have been applied to hindered rotations of adsorbates parallel to surfaces, and we do that here for the first time. The method of Pitzer and Gwinn[11] was also extended to hindered translations by Hill.[4] Here we improve that approximation for hindered translations in a way analogous to how Goddard's group[12] improved the approximation of Pitzer and Gwinn[11] for hindered rotations. We apply both these improved approximations to motions of adsorbates parallel to surfaces to estimate adsorbate entropies.

To implement these approximations for specific cases, to test their general accuracy, and to assess qualitative trends in their results, we utilize DFT with periodic boundary conditions and the climbing image nudged elastic band method (CI-NEB)[13−15] to estimate rotational and translational barrier heights and their periodicities. The standard-state molar entropies for adsorbed methane, ethane, propane, and methanol on Pt(111) are estimated in this way and found to agree very well with experimental values (1.0, 1.3, 0.5, and 1.7 R, respectively, less than the experimental values, which average 14 R). Other model systems with a wider range of physical properties (i.e., mass, lattice constant, moment of inertia, rotation barrier periodicity) are also studied, to study how they affect entropies of adsorbates. The results show that the 2D ideal lattice gas/harmonic oscillator model accurately predicts standard-state adsorbate entropies calculated with this improved model (within 0.23 R in every mode) when kT is less than the barriers to diffusion and rotation parallel to the surface and that the 2D ideal gas model accurately predicts these (to within 0.06 R per mode) when kT exceeds that barrier, provided that the vibrational frequencies for these modes are determined by fitting these barriers to a sine wave potential energy (as opposed to the usual DFT normal-mode analysis of the adsorbate's minimum-energy structure). However, the harmonic oscillator/lattice gas model severely overestimates the entropy when kT exceeds the barrier.

We discuss here only "ideal" adsorbates that have no adsorbate−adsorbate lateral interactions. It is well-known that such interactions can have huge effects on reaction energies and activation energies. These enthalpic effects often cause much bigger changes in equilibrium constants and rate constants than the entropic effects we discuss here, and so they cannot be neglected. Statistical mechanical treatments that include adsorbate−adsorbate interactions have been discussed in the literature, usually within the lattice gas/harmonic oscillator approximation.[16−20] Excluded volume is highly important and is naturally included in ideal 2D lattice gas models[21] and has been included in ideal 2D gas models as well.[22]

2. THEORY

2.1. Ideal 2D Hindered Translator: Partition Function.

The hindered translator method, adapted from Hill,[4] is used to calculate the partition function for a 2D hindered translator, q_{xy}. The adsorbates are considered to be ideal in that any adsorbate−adsorbate interactions are neglected. The partition function for z-motion, q_z, is assumed to be a harmonic oscillator (HO), contributing a factor q_z to the partition function given by the standard expression for a single HO vibrational mode of frequency ν_z.[4] This formulation is derived for dilute systems in which $N < M$ where N is the number of adsorbed species and M is the number of surface sites. Hill's approach is summarized below, but the notation has been changed to be consistent with Goddard's[12] hindered rotor notation.

In Hill's treatment the potential energy function for the hindered xy-motion is written as

$$V(x, y) = V_0 + \frac{W_x}{2}\left(1 - \cos\frac{2\pi x}{b}\right) + \frac{W_y}{2}\left(1 - \cos\frac{2\pi y}{b}\right) \quad (1)$$

DOI: 10.1021/acs.jpcc.5b11616
J. Phys. Chem. C 2016, 120, 9719−9731

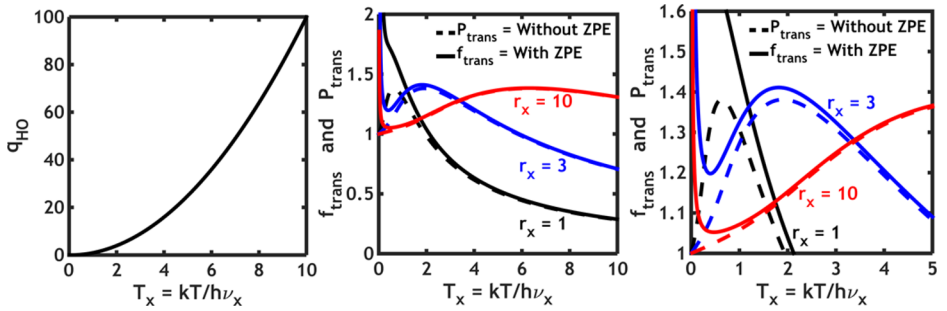

Figure 2. Left: The quantum harmonic oscillator partition function for two identical HO modes, x and y, from eq 5. Center: The hindered translator partition functions with and without the ZPE correction of eq 8 normalized to Mq_{HO}, i.e., $f_{trans} = q_{trans}/(Mq_{HO})$ and $P_{trans} = q_{xy}/(Mq_{HO})$, plotted versus temperature for three different r_x (r_x = 1, 3, 10). Right: An expanded plot of the lower temperature range. The ZPE correction factor only affects the values at low temperatures.

where V_0 is the potential energy at the minima; W_x and W_y are the translational energy barrier heights; and b is the nearest-neighbor distance between surface atoms, assumed to be the same in both directions. For simplicity, the barrier is also assumed to be the same in both x and y directions, so $W_x = W_y$ here, though these assumptions are easy to change in the end result. At low temperatures, the adsorbate experiences localized adsorption and vibrates about the minima with a frequency (where the force constant is obtained from the second derivative of the potential versus distance at the minimum) equal to

$$\nu_x = \nu_y = \left(\frac{W_x}{2mb^2}\right)^{1/2} \tag{2}$$

where m is its mass. At high temperatures, the adsorbate instead experiences free translation. At intermediate temperatures there is a transition from one extreme kind of adsorption to the other. During this transition, the xy-partition function can be written as

$$q_{xy} = q_{classical} \cdot \frac{q_{HO}}{q_{HO-classical}} \tag{3}$$

in which $q_{classical}$ is the classical partition function; q_{HO} is the quantum harmonic oscillator partition function; and $q_{HO\text{-}classical}$ is the classical harmonic oscillator partition function. The classical partition function is

$$q_{classical} = M(\pi r_x T_x)\exp\left[-\frac{r_x}{T_x}\right] I_0^2\left[\frac{r_x}{2T_x}\right] \tag{4}$$

where M is the number of surface sites; r_x is the ratio of the energy barrier height to the vibrational frequency times Planck's constant, $r_x = W_x/h\nu_x$; and the dimensionless temperature T_x is $T_x = kT/h\nu_x$. I_0 is the zero-order modified Bessel function of the first kind. The quantum partition function for a single harmonic oscillator oscillating independently in two identical directions is

$$q_{HO} = \left(\frac{\exp\left[-\frac{1}{2T_x}\right]}{1-\exp\left[-\frac{1}{T_x}\right]}\right)^2 \tag{5}$$

which at high temperature gives the classical limit

$$q_{HO-classical} = T_x^2 \tag{6}$$

Substitution of eqs 4–6 into eq 3 gives the same final result as Hill[4]

$$q_{xy} = \frac{M\left(\frac{\pi r_x}{T_x}\right)\exp\left[-\frac{r_x}{T_x}\right]\exp\left[-\frac{1}{T_x}\right] I_0^2\left[\frac{r_x}{2T_x}\right]}{\left(1-\exp\left[-\frac{1}{T_x}\right]\right)^2} \tag{7}$$

The M here could be replaced by $M = \mathcal{A}/b^2$ (area/(nearest neighbor distance)^2)for a surface with 4-fold symmetry (like FCC(100) faces) or by $M = \mathcal{A}/\left(\frac{\sqrt{3}}{2}b^2\right)$ for a surface with 3-fold symmetry (like FCC(111)), thus showing that q_{xy} is proportional to surface area, $\mathcal{A}$, just as for an ideal 2D gas.

This partition function is accurate at higher temperatures but gives an incorrect zero-point energy contribution at lower temperatures, as pointed out by McClurg, Flagan, and Goddard[12] for the nearly identical expression for hindered rotors. In the similar treatment of hindered rotors by McClurg et al.[12] (see above), they adopted the Padé approximant for ΔE^{zp} to account for the overestimation of the zero-point energy in the harmonic oscillator function. Using a similar approach for the translator here gives

$$q_{trans} = q_{xy}\exp\left[2\frac{\Delta E^{zp}}{kT}\right] \tag{8}$$

where

$$\Delta E^{zp} = \frac{h\nu_x}{2+16r_x} \tag{9}$$

The factor of 2 in eq 8 comes from the two degrees of freedom, x and y, which we assume here to have identical potential energy versus distance. Substituting for T_x, this simplifies to

$$q_{trans} = q_{xy}\exp\left[\frac{2}{(2+16r_x)T_x}\right] = \frac{M\left(\frac{\pi r_x}{T_x}\right)\exp\left[-\frac{r_x}{T_x}\right]\exp\left[-\frac{1}{T_x}\right] I_0^2\left[\frac{r_x}{2T_x}\right]}{\left(1-\exp\left[-\frac{1}{T_x}\right]\right)^2}\exp\left[\frac{2}{(2+16r_x)T_x}\right] \tag{10}$$

Defining an interpolation function f_{trans} as the ratio of the translational partition function to its (quantum) harmonic oscillator partition function, analogous to the hindered rotor interpolation function of McClurg et al. for internal rotations in molecules,[12] gives

DOI: 10.1021/acs.jpcc.5b11616
J. Phys. Chem. C 2016, 120, 9719–9731

$$f_{trans} = \frac{q_{trans}/M}{q_{HO}} \tag{11}$$

Here, q_{trans} is divided by M in this definition of f_{trans} since q_{trans} refers to the whole surface with M sites, whereas q_{HO} is defined here for a single harmonic oscillator site. This interpolation function can be seen by dividing eqs 10 and 5 above to equal

$$f_{trans} = P_{trans} \exp\left[\frac{2}{(2 + 16r_x)T_x}\right] \tag{12}$$

where

$$P_{trans} = \frac{q_{xy}}{Mq_{HO}} = \frac{\pi r_x}{T_x} \exp\left[-\frac{r_x}{T_x}\right] I_0^2\left[\frac{r_x}{2T_x}\right] \tag{13}$$

Figure 2 shows a plot of f_{trans} and P_{trans}, which is the hindered translator partition function normalized by Mq_{HO} versus temperature for different r_x values, with and without this zero-point energy correction. This only makes much difference at low temperatures.

2.2. Hindered Rotor: Partition Function. Here we consider only the hindered rotation of the whole adsorbate about an axis perpendicular to the surface. (On a rough or faceted surface, this could be the *local* surface normal.) The treatment of a hindered rotation is adopted from McClurg et al.[12] where the potential energy function for hindered rotation is

$$V(\phi) = \frac{W_r}{2}(1 - \cos n\phi) \tag{14}$$

where W_r is the energy barrier height for rotation and n is the number of equivalent minima in a full rotation. At low temperatures the harmonic oscillator frequency is

$$\nu_r = \frac{\omega}{2\pi} = \frac{1}{2\pi}\left(\frac{n^2 W_r}{2I}\right)^{1/2} \tag{15}$$

where I is the reduced moment of inertia given by

$$I = \sum_i m_i d_i^2 \tag{16}$$

where m_i is the mass of each adsorbate atom and d_i is the distance in the x–y plane from the center of each adsorbate atom to the axis about which the adsorbate is being rotated. Unlike in gas-phase rotation, this axis of rotation may not necessarily pass through the center of mass of the adsorbate since it might, for example, be attached most strongly to the surface through a bond nearer to one end of the adsorbate and rotate about that bond. Similarly to the hindered translator, the ratio of the energy barrier height to the harmonic oscillator frequency times Planck's constant, r_r, is defined as $r_r = W_r/h\nu_r$, and the dimensionless temperature, T_r, is $T_r = kT/h\nu_r$.

The quantum harmonic oscillator partition function in this case is

$$q_{HO} = \frac{\exp\left[-\frac{1}{2T_r}\right]}{1 - \exp\left[-\frac{1}{T_r}\right]} \tag{17}$$

which is identical in form to eq 5 above for translators, except that eq 5 is for two such modes, so it is squared there. Defining an interpolation function f_{rot} following McClurg et al.,[12] just as for hindered translations above, gives

$$f_{rot} = \frac{q_{rot}}{q_{HO}} \tag{18}$$

where McClurg et al.[12] showed that

$$f_{rot} = P_{rot} \exp\left[\frac{\Delta E^{zp}}{kT}\right] = P_{rot} \exp\left[\frac{1}{(2 + 16r_r)T_r}\right] \tag{19}$$

wherein they adopted the Padé approximant for ΔE^{zp} to account for the overestimation of the zero-point energy in the harmonic oscillator function. P_{rot} is the earlier approximation of q_{rot}/q_{HO} introduced by Pitzer and Gwinn[11] that did not include this correction and is given by[12]

$$P_{rot} = \left(\frac{\pi r_r}{T_r}\right)^{1/2} \exp\left[-\frac{r_r}{2T_r}\right] I_0\left[\frac{r_r}{2T_r}\right] \tag{20}$$

The full rotational partition function is then

$$q_{rot} = f_{rot} \times q_{HO} = \frac{\left(\frac{\pi r_r}{T_r}\right)^{1/2} \exp\left[-\frac{r_r}{2T_r}\right] \exp\left[-\frac{1}{2T_r}\right] I_0\left[\frac{r_r}{2T_r}\right]}{\left(1 - \exp\left[-\frac{1}{T_r}\right]\right)} \exp\left[\frac{1}{(2 + 16r_r)T_r}\right] \tag{21}$$

This now looks very similar to the expression for the partition function for hindered translation, with ${q_{rot}}^2 = q_{trans}/M$, except for the subtle differences in the definitions of their parameters r_i and T_i. As seen by comparing eqs 19 and 20 with eqs 12 and 13, f_{trans} is just ${f_{rot}}^2$, which is squared because there are two translational modes but only a single rotational mode.

We have assumed above that the rotor is *asymmetric*. For *symmetric* rotors, the expressions above for q_{rot} must be divided by the symmetry number (e.g., 2 for a linear alkane rotating about its center of mass).[23]

2.3. Thermodynamic Functions. We assume here that the densities of states for the solid's modes are not changed upon adsorption. The total partition function for the adsorbate is given by

$$q_{ad} = q_{trans} \cdot q_{rot} \cdot q_z \cdot q_{int\text{-}vib} \tag{22}$$

where $q_{int\text{-}vib}$ is the partition function for all the internal vibrations of the adsorbate, including the vibration(s) of the whole adsorbate about the two rotational axes parallel to the surface (i.e., cartwheel-like rotations that become vibrations upon adsorption). (Linear adsorbates lying flat on the surface have only one such axis.) The number of such internal vibrational modes is three times the number of atoms in the molecule minus four (since there are two hindered translations, one hindered rotation parallel to the surface (i.e., helicopter-like rotation), and one vibration of the whole adsorbate perpendicular to the surface). Since the adsorbates are identical, noninteracting, and indistinguishable, they follow Boltzmann statistics. Therefore, the Helmholtz free energy A is given as

$$A = -NkT \ln\left[\frac{q_{ad} e}{N}\right] = -NkT \ln\left[\frac{(q_{ad}/\mathcal{A})e}{(N/\mathcal{A})}\right] = -NkT \ln\left[\frac{(q_{ad}/M)e}{(N/\mathcal{A})b^2}\right] \tag{23}$$

DOI: 10.1021/acs.jpcc.5b11616
J. Phys. Chem. C 2016, 120, 9719–9731

Expanding q_{ad} above and separating terms gives that

$$A = A_{trans} + A_{rot} + A_z + A_{int\text{-}vib} \quad (24)$$

where each contribution A_i for q_{rot}, q_z, and $q_{int\text{-}vib}$ is given by

$$A_i = -NkT \ln q_i \quad (25)$$

except A_{trans}, which is instead

$$A_{trans} = -NkT \ln\left[\frac{(q_{trans}/\mathcal{A})e}{(N/\mathcal{A})}\right] = -NkT \ln\left[\frac{(q_{trans}/M)e}{(N/\mathcal{A})b^2}\right] \quad (26)$$

In eqs 23 and 26 we assumed $\mathcal{A} = Mb^2$, which is only valid for a surface with 4-fold symmetry (like FCC(100) faces). For a surface with 3-fold symmetry (like FCC(111)), one must replace this with $\mathcal{A} = M\left(\frac{\sqrt{3}}{2}b^2\right)$ instead. The same applies in eqs 29 and 38 below. This also applies to b^2 in eq 2 for the frequency, where now $\nu_x = \left(\frac{W_x}{2m(\sqrt{3}/2 * b^2)}\right)^{1/2}$. This form is used in our calculations for Pt(111) described below. An equation similar to eq 24 was presented by Kreuzer[17] but without the hindered translator/hindered rotor corrections discussed below.

If we set the zero-energy reference as the zero-point vibrational energy of the adsorbate, every vibrational mode of frequency ν_i contributes an amount to A of[23]

$$A_{HO,i} = NkT\left(\ln\left[1 - \exp\left[-\frac{h\nu_i}{kT}\right]\right]\right) = NkT\left(\ln\left[1 - \exp\left[-\frac{1}{T_i}\right]\right]\right) \quad (27)$$

where we define the dimensionless temperature, T_i, as $T_i = kT/h\nu_i$ (not to be confused with the so-called vibrational temperature, $h\nu_i/k$). Every hindered translational or hindered rotational mode i contributes this same amount plus an additional amount equal to[12]

$$\Delta A_i = -NkT \ln f_i = NkT\left(\frac{-1}{(2 + 16r_i)T_i} + \frac{r_i}{2T_i} - \ln\left[\left(\frac{\pi r_i}{T_i}\right)^{1/2} I_0\left[\frac{r_i}{2T_i}\right]\right]\right) \quad (28)$$

Note that the 2D hindered translator must include two such contributions, for x and y motion, which are equal to each other since we assumed that W and b are identical in the x and y directions, such that $f_{trans} = f_x f_y = f_x{}^2$.

In addition, these two hindered translator modes, when grouped together, contribute an additional amount to A_{trans} and A equal to

$$A_1 = -NkT(1 - \ln[b^2(N/\mathcal{A})]) = NkT(\ln\theta - 1) \quad (29)$$

This arises from the factor $e/((N/\mathcal{A})b^2) = e/\theta$ in eqs 23 and 26, where $\theta = (N/\mathcal{A})/(M/\mathcal{A})$ is the fractional coverage. For standard-state free energy, one must use the standard-state surface concentration for $N/\mathcal{A}$ here. (As discussed above, this equation is valid for a surface with 4-fold symmetry. For surfaces with 3-fold or 6-fold symmetry, replace b^2 with $\frac{\sqrt{3}}{2}b^2$.) As shown elsewhere,[21] A_1 has essentially the same quantitative value versus θ as the contribution of the configurational degeneracy (configurational entropy) to the free energy of an ideal 2D *lattice* gas except at high θ (>0.05), but it arises from fundamentally different reasons.

For standard-state thermodynamic values, we simply use the standard state concentration, $(N/\mathcal{A})^0$, for $(N/\mathcal{A})$ here. We have shown previously that the standard value $(N/\mathcal{A})^0$ is most convenient when taken as[21]

$$\left(\frac{N}{\mathcal{A}}\right)^0 = e^{1/3}\left(\frac{N_A}{V^0_{gas}}\right)^{2/3} = 1.40\left(\frac{N_A}{V^0_{gas}}\right)^{2/3} \quad (30)$$

where (N_A/V^0) is the standard-state concentration of the 3D ideal gas, which is defined as its concentration at the standard pressure of 1 bar and T. This is given by the ideal gas law as 1 bar/(kT), which at 298 K is one mole per 24.8 L. This sets the standard-state surface concentration as 1.17×10^{13} cm^{-2} at 298 K.

Substituting the ideal gas law expressions for $\left(\frac{N_A}{V^0_{gas}}\right) = \left(\frac{N_A\ 1\ bar}{RT}\right)$ gives

$$\left(\frac{N}{\mathcal{A}}\right)^0 = 1.40\left(\frac{N_A\ 1\ bar}{RT}\right)^{2/3} \quad (31)$$

We proved[21] that choosing this standard concentration is equivalent to choosing a standard state such that the translational contribution to the standard molar entropy is 2/3 of that for the 3D ideal gas. This is a convenient and intuitive choice since it has 2/3 the number of translational degrees of freedom. We also proved[21] that, to similarly ensure that the translational contribution to the standard molar entropy of an adsorbate treated as an ideal 1D gas is 1/3 of that for the 3D ideal gas, its standard-state concentration must be $e^{2/3}$ times the 1/3 power of the standard-state concentration of a 3D ideal gas. These choices have an intuitive advantage when estimating standard reaction entropies and activation entropies when calculating equilibrium constants and rate constants for surface reactions.[21]

The internal energy E is given in Boltzmann statistics by[4,23]

$$E = NkT^2\left(\frac{d \ln q_{ad}}{dT}\right)_{\mathcal{A}} \quad (32)$$

Similarly, every HO vibrational mode contributes an amount to E (relative to its zero-point energy as the zero reference energy) of[23]

$$E_{HO,i} = Nh\nu_i\left(\frac{1}{\exp[h\nu_i/kT] - 1}\right) = NkT\left(\frac{1/T_i}{\exp[1/T_i] - 1}\right) \quad (33)$$

Every hindered translational and hindered rotational mode contributes this plus an additional amount to the internal energy equal to

$$\Delta E_i = NkT^2\left(\frac{d \ln f_i}{dT}\right)_{\mathcal{A}} = NkT\left(-\frac{1}{2} - \frac{1}{(2 + 16r_i)T_i} + \frac{r_i}{2T_i}\left(1 - \frac{I_1\left[\frac{r_i}{2T_i}\right]}{I_0\left[\frac{r_i}{2T_i}\right]}\right)\right) \quad (34)$$

DOI: 10.1021/acs.jpcc.5b11616
J. Phys. Chem. C 2016, 120, 9719−9731

This is identical to the result for the contribution of f_{rot} to E as given by McClurg, Flagan, and Goddard,[12] except they had a sign error on the term $(1 - I_1[r_i/2T_i]/I_0[r_i/2T_i])$. Again for the 2D hindered translator, there are two such contributions, equal to each other since we assume that W and b are identical in x and y here.

The entropy is then given by[4]

$$S = \frac{E - A}{T} \tag{35}$$

Every vibrational mode of frequency ν_i thus contributes an amount to S equal to[23]

$$S_{HO,i} = Nk\left(\frac{h\nu_i/kT}{\exp[h\nu_i/kT] - 1} - \ln\left[1 - \exp\left[-\frac{h\nu_i}{kT}\right]\right]\right)$$
$$= Nk\left(\frac{1/T_i}{\exp[1/T_i] - 1} - \ln\left[1 - \exp\left[-\frac{1}{T_i}\right]\right]\right) \tag{36}$$

Every hindered translational or hindered rotational mode i contributes this same amount plus an additional amount equal to[12]

$$\Delta S_i = \frac{\Delta E_i - \Delta A_i}{T}$$
$$= Nk\left(-\frac{1}{2} - \frac{r_i}{2T_i}\frac{I_1\left[\frac{r_i}{2T_i}\right]}{I_0\left[\frac{r_i}{2T_i}\right]} + \ln\left[\left(\frac{\pi r_i}{T_i}\right)^{1/2} I_0\left[\frac{r_i}{2T_i}\right]\right]\right) \tag{37}$$

Finally, the two translational modes taken together contribute an additional, concentration-related amount to the entropy (arising from A_1) equal to[21]

$$S_1 = -Nk(\ln[b^2(N/\mathcal{A})] - 1) = -Nk(\ln\theta - 1) \tag{38}$$

For standard-state entropies, one must use the standard-state surface concentration for $N/\mathcal{A}$ here. (This equation is valid for a surface with 4-fold symmetry. For surfaces with 3-fold or 6-fold symmetry, replace b^2 with $\frac{\sqrt{3}}{2}b^2$.) As noted above, S_1 has essentially the same value as the configurational entropy of an ideal 2D lattice gas except at high θ (>0.05), but it arises from fundamentally different reasons. When an adsorbate is treated as an ideal 2D gas, it has the same concentration-dependent contribution S_1 as in eq 38, and the remaining, concentration-independent part of its entropy is given by $S - S_1 = R\ln[(qe/\mathcal{A})/(M/\mathcal{A})]$, where $M/\mathcal{A}$ is the saturation concentration used to define its relative coverage, $\theta = (N/\mathcal{A})/(M/\mathcal{A})$.[21] For ideal 2D monatomic gases, this gives $S - S_1 = R\ln[(2\pi mkTe/h^2)/((M/\mathcal{A}))]$.

We verified that these equations above give the same entropy as that for an ideal 2D gas for the case of a monatomic gas in the limit of extremely small diffusion barrier, W.

3. COMPUTATIONAL METHODS

The electronic structure calculations for each adsorbed species on Pt(111) and the energy barriers for their rotation and translation were calculated utilizing density functional theory (DFT) via the Vienna Ab-initio Simulation Package (VASP).[24−27] The projector augmented wave (PAW) method[28,29] was used to represent the core electrons. The exchange correlation potential and energy were described by the generalized gradient approximation (GGA) as defined by the Perdew−Burke−Ernzerhof (PBE) functional.[30,31] Calculations that included van der Waals (vdW) forces used the D3 method of Grimme.[32]

The supercell was a 3 × 3 × 3 Pt(111) slab with 20 Å of vacuum space and periodic boundary conditions. Initially only the bottom layer of Pt was held fixed, while the top two layers were allowed to relax, simulating a surface. Then all Pt atoms were held fixed, and one molecule was allowed to adsorb on the Pt surface, giving a coverage of $\theta = 1/9$ monolayer. Relaxing the top two layers of the surface decreases the adsorption energy of methanol on the Pt slab by 5×10^{-3} eV with vdW and by 4×10^{-4} eV without vdW and increases the barrier heights for translations by 0.01 and 0.02 eV with and without vdW, respectively. The rotational barriers were not affected significantly by the relaxation of the surface, but these barriers were already very small. These are very small relative differences in the barrier heights (e.g., <5% for diffusion using vdW), so we neglected relaxation for the barrier height calculations reported here. The adsorbed molecules included methanol, methane, ethane, and propane. The two lowest-energy structures for adsorbed propane have different adsorbed configurations, one with its secondary (C_2) carbon atom closest to a Pt atom and another with its primary (C_1) carbon atoms closer to Pt atoms. The energy difference between the two adsorbed configurations of propane was only 0.02 eV with vdW and 0.01 eV without vdW, so both were included. The lowest energy adsorption site for all molecules calculated was with either a C or O atom sitting very near the atop site of a metal atom, such that there are six essentially equal barriers to rotation parallel to the surface (i.e., one every 60°).

The kinetic energy cutoff for the Kohn−Sham orbitals was 410 and 400 eV for calculations with and without vdW interactions, respectively. Increasing the cutoff energies to 500 eV only changes the adsorption energy of methanol by 6×10^{-4} eV with vdW and 1×10^{-3} eV without vdW. Plane-wave calculations were employed using the Monkhorst−Pack method[33] with 5 × 5 × 1 special k points. Increasing the number of k points to 7 × 7 × 1 changes the adsorption energy by 0.03 and 0.01 eV with and without vdW, respectively. All simulations were relaxed until the forces were below 0.02 eV/Å.

The minimum energy path (MEP) and transition states for translation and rotation of each adsorbate were calculated by the CI-NEB method.[13,14] Seven images were calculated between all initial and final states. Translations were calculated as the translations from atop site to an adjacent atop site, and rotations were simulated as a 120° rotation around the z-axis through the adsorption site. Initial and saddle point configurations for all calculations with vdW are provided in the Supporting Information. In some cases, the minimum energy path for rotation has the adsorbate rotating about one Pt atom and not about the adsorbate's center of mass. For this reason, the distance term in the reduced moment of inertia, eq 16, is calculated as the distance in the x−y plane from each adsorbate atom to the center of the Pt atom about which the adsorbate rotates. The calculated lattice constants for Pt were 3.92 and 3.97 Å with and without including the vdW correction, respectively, compared to 3.92 Å determined experimentally.[34]

Vibrational frequencies were determined from the eigenvalues of the Hessian matrix for the minima energy configuration of each adsorbate on the surface. Two displacements were used for each direction and atom with a step size of 0.01 Å for all atoms in the adsorbate, while the surface atoms were held fixed.

DOI: 10.1021/acs.jpcc.5b11616
J. Phys. Chem. C 2016, 120, 9719−9731

Table 1. Summary of DFT Calculations of Energy Barriers (W_x), Vibrational Frequencies (ν_x), and Their Ratios (r_x) for the Hindered Translation of Several Adsorbates on a Pt(111) Surface

adsorbate	vdW included?	energy barrier W_x (eV)	mass m (amu)	frequency ν_x (s^{-1})	$r_x = W_x/(h\nu_x)$	adsorption energy E_{ads} (eV)
methanol	yes	0.294	32	2.58×10^{12}	27.5	−0.306
methanol	no	0.218	32	2.20×10^{12}	24.0	−0.728
propane (C_2)	yes	0.091	44	1.23×10^{12}	18.0	−0.062
propane (C_2)	no	0.041	44	8.12×10^{11}	12.2	−0.656
propane (C_1)	yes	0.066	44	1.05×10^{12}	15.3	−0.054
propane (C_1)	no	0.023	44	6.13×10^{11}	9.2	−0.637
ethane	yes	0.049	30	1.09×10^{12}	10.9	−0.045
ethane	no	0.020	30	6.81×10^{11}	7.0	−0.458
methane	yes	0.006	16	5.36×10^{11}	2.9	−0.037
methane	no	0.005	16	4.50×10^{11}	2.5	−0.270

Table 2. Summary of DFT Calculations of Energy Barriers (W_r), Vibrational Frequencies (ν_r), and Their Ratios (r_r) for the Hindered Rotation of Several Adsorbates on a Pt(111) Surface

adsorbate	vdW included?	energy barrier W_r (eV)	reduced moment of inertia I (amu*Å^2)	frequency ν_r (s^{-1})	$r_r = W_r/(h\nu_r)$
methanol	yes	0.002	22.3	6.94×10^{11}	0.85
methanol	no	0.001	21.1	5.29×10^{11}	0.61
propane (C_2)	yes	0.011	104.1	6.86×10^{11}	3.9
propane (C_2)	no	0.002	69.0	3.33×10^{11}	1.3
propane (C_1)	yes	0.046	165.9	1.10×10^{12}	10.0
propane (C_1)	no	0.022	162.0	7.66×10^{11}	6.8
ethane	yes	0.018	73.4	1.03×10^{12}	4.2
ethane	no	0.0006	37.8	2.63×10^{11}	0.55
methane	yes	0.0008	8.77	6.26×10^{11}	0.30
methane	no	0.0001	3.35	3.99×10^{11}	0.07

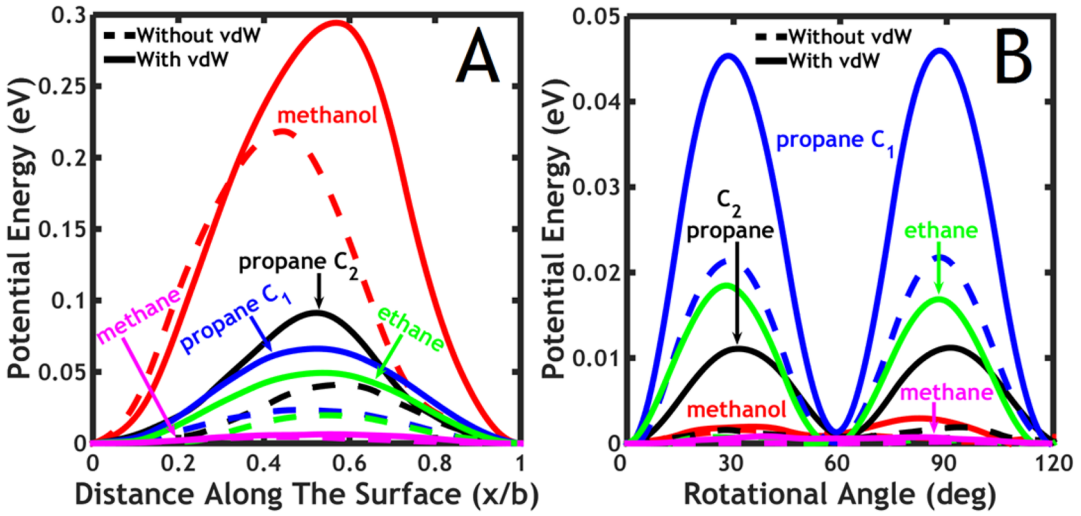

Figure 3. Calculated energy barrier versus coordinate of different adsorbates on Pt(111) for: (A) hindered translations and (B) hindered rotations.

This new approach for calculating partition functions and entropies for adsorbates within the ideal hindered translator/hindered rotor model will be implemented into the thermochemistry module of ASE[35] as well as into CatMAP.[36]

4. RESULTS AND DISCUSSION

4.1. Comparison of Predicted Entropies of Small Adsorbates on Pt(111) to Experiments. To test the accuracy of the method, we model here several molecular adsorbates (methane, ethane, propane, and methanol) on the Pt(111) surface, systems for which the experimental standard-state entropy has been reported.[3,37] All adsorbates studied adsorb on atop sites, so each adsorbate has six equivalent minima in a full rotation (i.e., $n = 6$). Translational energy barrier heights and rotational energy barrier heights were determined by DFT calculations using the climbing image nudge elastic band (CI-NEB) method and are listed in Tables 1 and 2. These barrier heights were then used together with the site periodicities to fit the potential energy versus coordinate to cosine waves (i.e., eq 1 or 14), from which we calculated the corresponding translational and rotational frequencies using eqs 2 and 15 and the ratios of the energy barrier height to the vibrational frequency, r_x and r_r. This approach has been used previously to better estimate the frequencies for hindered translations of adsorbates.[5,7] For the systems studied here, these frequencies were generally lower than those that came directly

DOI: 10.1021/acs.jpcc.5b11616
J. Phys. Chem. C 2016, 120, 9719−9731

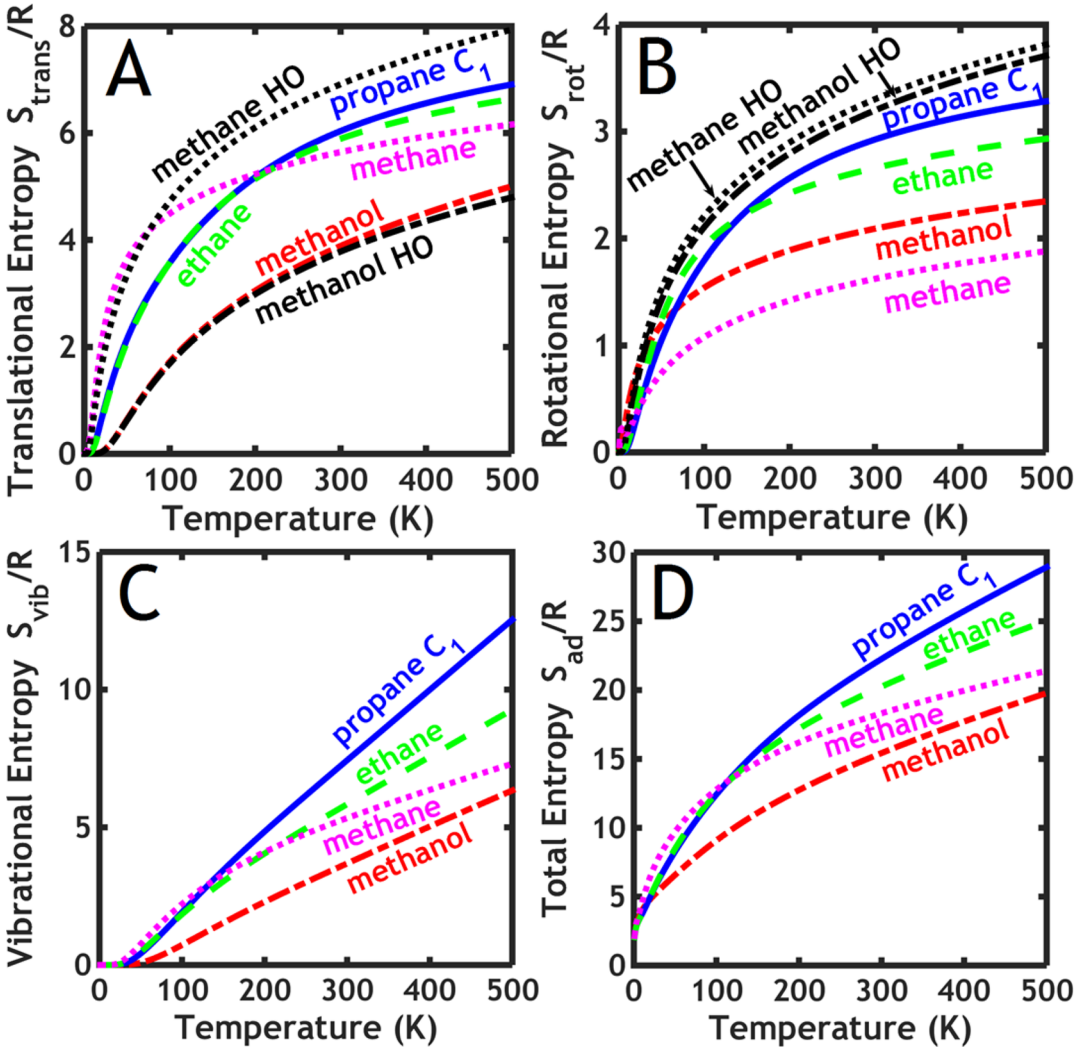

Figure 4. Entropy contributions as a function of temperature for: (A) two hindered translations (not including the concentration-related part, S_1, see Table 3), (B) the hindered rotation, (C) the 3n-3 vibrations, which include all internal vibrations and the *z*-vibration of the whole adsorbate, and (D) the total entropy. All curves are computed using DFT with vdW corrections included. Shown for comparison in A and B are the predictions of the harmonic oscillator approximation for methane and methanol (curves labeled "HO").

from the normal-mode analysis, with an average ratio of 0.70 ± 0.41 for calculations with vdW corrections. These barriers and their ratios to $h\nu_i$ are also listed in Tables 1 and 2. The translational ratios $r_x = W_x/h\nu_x$ vary from $r_x = 2-28$, while the ratios for rotations range from $r_r = 0-10$. The ratios of W_x and W_r to the adsorption energy averaged 0.09 and 0.008, respectively, for DFT using vdW corrections, with standard deviations slightly larger than these averages.

The energy versus coordinate for all adsorbates' hindered translations and rotations is shown in Figure 3, with geometries at the initial state and transition state presented in the Supporting Information. Their corresponding contributions to the adsorbate's total standard molar entropy are shown versus temperature in Figure 4, along with the contributions from the 3n-3 vibrations, which include all internal vibrations and the *z*-vibration of the whole adsorbate. We have assumed here that the three lowest vibrational frequencies which come directly out of the DFT normal-mode calculations correspond to the two hindered translations and the hindered rotation. We verified that this is qualitatively correct for the case of adsorbed methanol by visualizing its three lowest-frequency normal-mode motions (calculated including vdW), although it was also clear that these modes include some other minor contributing coordinates. Thus, the frequencies used for the frequencies for the remaining 3n-3 vibrations were taken from the remainder of those calculated frequencies, and these lowest three frequencies were discarded (i.e., replaced with hindered translation and hindered rotation partition functions).

Also shown in Figure 4 are the predictions of the HO approximation for the entropy contributions from *xy* motions (A) and rotation (B) parallel to the surface for adsorbed methane and methanol. As seen, the HO approximation severely overestimates the rotational entropy at high temperatures for both these adsorbates and the translational entropy at high temperature for methane. This can be understood with the equipartition theorem: The molar heat capacity of a harmonic oscillator is *R* in the high-temperature limit, but it is only 1/2 *R* for a free translator or free rotor. As shown below, the entropy of the hindered translator and hindered rotor reach the free translator (ideal 2D gas) and free rotor limits as soon as kT exceeds the barrier height, W. Since kT never exceeds the translational barrier for methanol on this plot, this problem is not seen for methanol in Figure 4A. For this same reason (i.e., kT never exceeds the barrier by much), the HO approximation

DOI: 10.1021/acs.jpcc.5b11616
J. Phys. Chem. C 2016, 120, 9719−9731

Table 3. Separation of the (1) Concentration-Related, (2) Hindered Translational, (3) Hindered Rotational, and (4) Vibrational Entropy Contributions to the Standard-State Molar Entropy of the Probe Adsorbates on a Pt(111) Surface at the Temperature of the Peak Maximum for Temperature-Programmed Desorption, T_{max}, Using Energy Barriers from DFT with and without vdW Corrections[a]

	methanol		propane (C_2)		propane (C_1)		ethane		methane	
T_{max} (K)	210		139		139		106		63	
vdW included	yes	no	yes	no	yes	no	yes	no	yes	no
$W_x/(kT_{max})$	16.3	12.1	7.62	3.42	5.53	1.95	5.40	2.15	1.17	0.844
$W_r/(kT_{max})$	0.135	0.074	0.930	0.145	3.81	1.80	1.94	0.065	0.144	0.022
concentration related S_1/R	5.6	5.6	5.3	5.3	5.3	5.3	5.2	5.1	4.8	4.8
hindered translations S_{trans}/R	3.2	3.5	3.9	5.0	4.3	5.5	3.7	4.8	3.9	4.0
harmonic oscillator model S_{trans}/R	3.1	3.4	3.7	4.5	4.0	5.1	3.4	4.4	3.8	4.2
hindered rotation S_{rot}/R	1.9	1.9	1.7	1.6	2.2	2.5	2.0	1.8	0.9	0.4
harmonic oscillator model S_{rot}/R	2.8	3.1	2.4	3.2	2.0	2.3	1.8	3.1	1.8	2.2
3n-3 vibrations S_{vib}/R	2.4	2.6	3.0	3.9	3.1	4.5	2.0	3.0	1.2	1.2
total S_{ad}/R	13.1	13.6	14.0	15.8	15.0	17.9	12.9	14.7	10.8	10.4
experimental S_{ad}/R	14.7		15.5		15.5		14.2		11.7	
std-state conc[21] $(N/\mathcal{A})^0$ (m^{-2})	1.48×10^{17}		1.95×10^{17}		1.95×10^{17}		2.33×10^{17}		3.30×10^{17}	

[a]The hindered translational and rotational entropies both include the zero-point energy corrections of eqs 8 and 19. Also shown for these hindered translator and hindered rotor modes are the entropies predicted by the harmonic oscillator approximation. The vibrational contribution includes all 3n-3 other normal modes of the adsorbates determine by DFT. Also shown is the total molar entropy and, for comparison, the experimental value as well as the standard-state concentration

does better for the other adsorbates below 500 K in both translational and rotational entropy (not shown). Less severe is the underestimation of the HO approximation at intermediate and low temperatures (i.e, when kT is ~10% of the barrier), but it works well at very low temperatures. This is discussed in more detail below.

The standard-state entropies of the adsorbed species are compared to experimental values in Table 3 and Figure 5. The

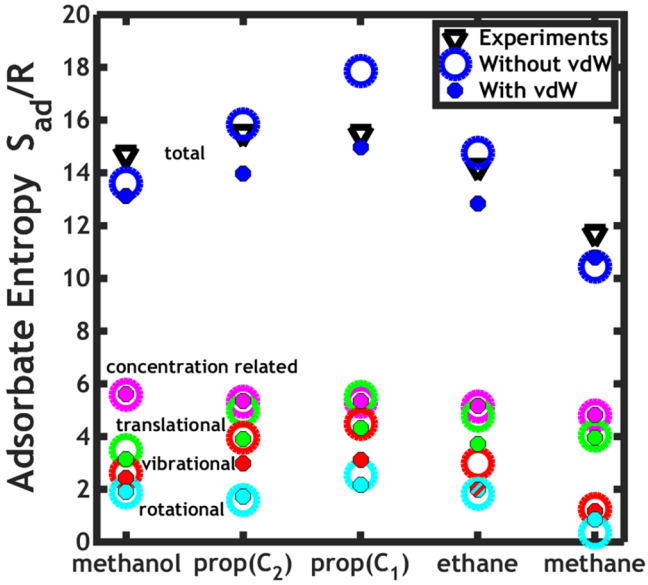

Figure 5. Plot of standard-state entropies determined for different adsorbates on Pt(111) through the hindered translator and hindered rotor method compared to experimental standard-state entropies at the experimental peak maximum for temperature-programmed desorption. The temperature is 210 K for methanol, 139 K for propane, 106 K for ethane, and 63 K for methane. Experimental values are from refs 3 and 37. Also shown are the various contributions to the total entropy, as defined in Table 3. Values derived from DFT energies calculated both with and without vdW corrections are shown as dots and circles, respectively.

experimental entropies were reported only at one temperature for each adsorbate on Pt(111), which corresponds to the peak maximum in the experimentally reported temperature-programmed desorption (TPD) spectrum,[37] so the calculated entropies are also at that temperature for each adsorbate, as listed in Table 3. These values all correspond to the standard-state adsorbate concentration which sets the entropy of an ideal 2D monatomic gas equal to 2/3 the standard state entropy of the corresponding ideal 3D gas, i.e., approximately 1% of a monolayer.[21] Although not so clearly stated there, this was the standard state used for the experimental entropies[3,37] that are listed in Table 3.

The agreement between experiment and theory is excellent for the case where the energies were determined using DFT with vdW corrections, giving an average absolute value of the error of only 1.1 R or 8% for the four adsorbates (using the model for propane where it rotates about C_1). This increases to 1.3 R or 9% when using DFT without vdW corrections. The entropies were up to 3 R larger for calculations without vdW corrections compared to those with vdW corrections. This was almost entirely due to the larger translational entropies, which is due to the smaller translational barriers, W_x, for DFT without vdW, which in turn is associated with the smaller heats of adsorption without vdW corrections. There is no significant difference between the calculated entropies for the two different models used for propane rotation (i.e., about an end carbon atom (C_1) or central carbon atom (C_2)).

Standard-state adsorbate entropies (for both the stable adsorbed species and their transition states) calculated with this approach can be used together with transition-state theory to calculate rate constants and their pre-exponential factors for elementary reaction steps involving adsorbates.[37] The high accuracy of this approach for estimating adsorbate entropies implies that the pre-exponential factors determined using entropies estimated in this way should be quite accurate.

The various contributions to the standard-state entropy for each species are also presented in Table 3 and Figure 5. The dominant contributions are the concentration-related term (S_1) and the two hindered translations.

DOI: 10.1021/acs.jpcc.5b11616
J. Phys. Chem. C 2016, 120, 9719−9731

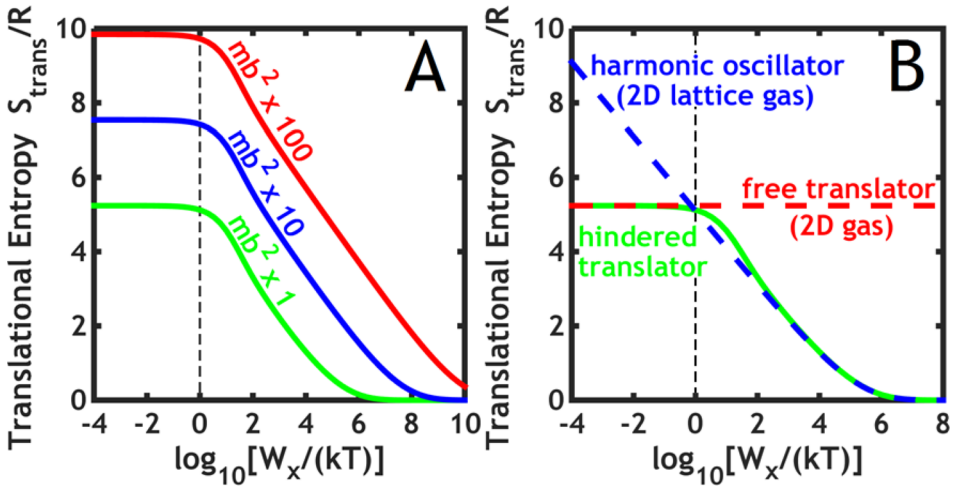

Figure 6. (A) Effect of the translational barrier height, W_x, on the translational contribution to the molar entropy ($S_{trans} - S_1$) at T = 106 K estimated using the hindered translator model for ethane on Pt(111) (where mb^2 = 2.30 amu*nm^2 = 3.82 × 10^{-45} kg*m^2, labeled "mb^2 × 1" here) and for adsorbate systems with values of mb^2 (mass times area per site) that are 10-fold and 100-fold larger than this. For ethane on Pt(111), the barrier estimated using DFT with vdW corrections is W_x = 7.90 × 10^{-21} J or 4.76 kJ/mol (W_x/k = 572 K), giving ν_x = 1.09 × 10^{12} s^{-1} ($h\nu_x/k$ = 52.4 K). (B) The translational contribution to the molar entropy ($S_{trans} - S_1$) of ethane on Pt(111) at T = 106 K versus $W_x/(kT)$ estimated from the hindered translator model, compared with that from the corresponding 2D harmonic oscillator model. The flat region on the left gives the same limiting entropy (at low $W_x/(kT)$) as the corresponding ideal 2D monatomic gas. (The concentration-dependent contribution, S_1, is not included in either curve.).

The S_1 value of 4.8 to 5.6 R here depends strongly on the choice of standard-state concentration, which we chose here as recommended in ref 21 such that the standard-state entropy of an ideal 2D monatomic gas (i.e., in the limiting case of unhindered translation where the barrier drops to zero) equals 2/3 of the entropy of the corresponding ideal 3D gas of the same mass at its standard state (i.e., at 1 bar pressure).[21] This standard state corresponds to approximately 1% of the maximum coverage. This S_1 contribution would drop to 1.7 R if a standard-state coverage of 1/2 the saturation coverage were chosen instead.[21] We chose the prior definition here to be consistent with the papers that reported the experimental entropies used here,[3,37] although that choice was only implied but never directly stated in those papers. It is also a value which gives a concentration-related contribution to the entropy (S_1) which is identical to the configurational entropy of an ideal lattice gas at the same standard-state surface concentration. We must admit that this difference of 3.1 to 3.9 R that arises from this (hidden) difference in standard-state concentrations was a large contributor to our earlier perception that the 2D lattice gas/harmonic oscillator model seriously underestimates adsorbate entropies.[21]

The difference between the hindered translator/hindered rotor entropy and that estimated within the 2D lattice gas HO approximation is given by eq 37 and shown in Table 3 at these experimental conditions. As seen in Table 3, the errors in the translational entropies using the HO/2D lattice gas approximation are rather small, averaging only 0.2 R per mode (x or y) for the four adsorbates using DFT with vdW corrections. The error in the HO approximation compared to the hindered rotor model is larger, often overestimating the entropy by over 1 R but still by less than 2 R. Thus, the HO approximation (i.e., using eq 36 but omitting eq 37) is moderately accurate at the temperatures of the experiments (but it severely overestimates entropies at higher temperatures—see below and Figure 4A and B above). A more important effect at the experimental temperatures is the use of frequencies in eq 36 that fit the energy minima and maxima to a cosine wave, as we have done here, instead of using the three lowest frequencies that come directly from the same DFT calculations, which are systematically higher. That latter approach leads to molar entropies that are lower by 1.5 R on average for the four adsorbates of Figure 5.

The entropies of these same three alkanes adsorbed on zeolite H−CHA at 303 to 313 K were estimated by Sauer's group with an approach that also goes beyond the harmonic oscillator approximation by including anharmonic effects and were found to agree well with experiments.[38] We used our new approach reported above to estimate the entropies of these alkanes on Pt(111) (with barriers estimated including vdW) but at the higher temperatures used in that paper. This provides a crude way to estimate the entropies of these adsorbates on that zeolite without doing DFT to get barrier heights on the zeolite, i.e., by assuming that the barriers for translation and rotation are the same as on Pt(111). In spite of this assumption, the entropies were found to be very close to those reported using Sauer's approach: 14.8 R vs 14.8 R for methane, 16.9 R vs 18.7 R for ethane, 19.0 R vs 21.6 R for propane (C1), and 17.8 R vs 16.9 R for propane (C2). These calculations were done at θ = 0.5 for direct comparison to the coverage used in Sauer's calculations. (Note that this is much higher than the coverage in Table 3 and thus gives entropies that are 3.7 R lower than the coverage of Table 3.) The approach used here is easier to implement than that developed by Sauer et al.[38]

4.2. Dependence of Adsorbate Entropy on System Parameters. To understand the qualitative dependences of the entropy upon the system parameters for the new hindered translator and hindered rotor models presented here, we calculated the translational and rotational contributions to the entropy of adsorbates for a wide variety of adsorbate parameters. Figure 6A shows how the translational contribution to the entropy for ethane on Pt(111) depends upon $W_x/(kT)$, the translational barrier normalized to kT, where T = 106 K, the experimental T_{max} for ethane on Pt(111). This is the curve

DOI: 10.1021/acs.jpcc.5b11616
J. Phys. Chem. C 2016, 120, 9719−9731

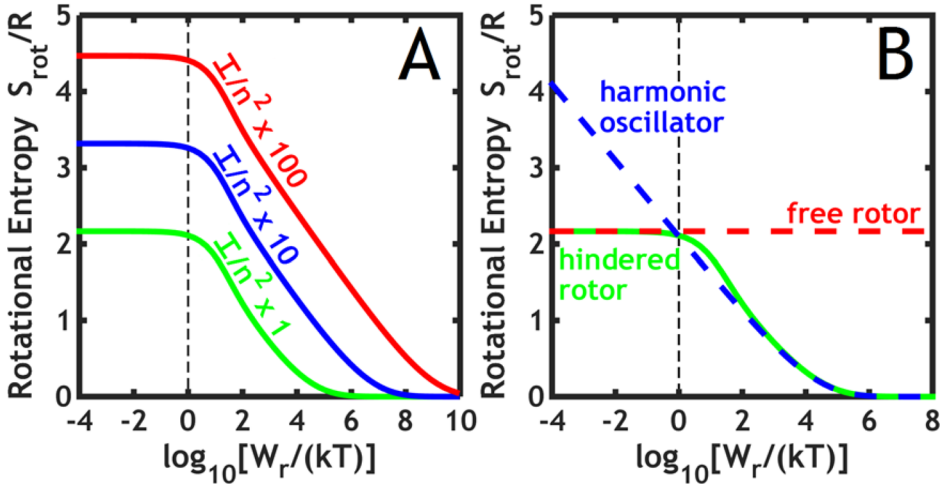

Figure 7. (A) Effect of the rotational barrier height, W_r, on the rotational contribution to the molar entropy at T = 106 K estimated using the hindered rotor model for ethane on Pt(111) (where I/n^2 is 0.0204 amu*nm^2 = 3.39 × 10^{-47} kg*m^2, labeled "$I/n^2 \times 1$" here) and for adsorbate systems with values of I/n^2 (reduced moment of inertia divided by the square of the number of energy barriers per rotation) that are 10-fold and 100-fold larger than this. For ethane on Pt(111), the barrier here was estimated using DFT with vdW corrections and is W_r = 2.83 × 10^{-21} J or 1.71 kJ/mol (W_r/k = 205 K), giving ν_r = 1.03 × 10^{12} s^{-1} ($h\nu_r/k$ = 49.4 K). (B) The rotational contribution to the molar entropy for ethane on Pt(111) at T = 106 K versus $W_r/(kT)$ estimated from the hindered rotor model, compared with that from the corresponding harmonic oscillator model. The flat region on the left gives the same limiting entropy (at low $W_r/(kT)$) as the corresponding free 1D rotor.

labeled "$mb^2 \times 1$". It is calculated using only eqs 36 and 37 and does not include the concentration-dependent part, S_1, from eq 38, so we will call it $S_{trans} - S_1$. As seen, this entropy is nearly constant when $W_x/(kT)$ is below 1 and then decreases with increasing $W_x/(kT)$, asymptotically approaching zero for large $W_x/(kT)$. The parameters m and b are always grouped together as mb^2 in the equations that determine S for the hindered translator. For a given value of $W_x/(kT)$, the translational entropy also increases with mb^2 (the adsorbate's mass times the area per site) as shown. The general shape of $S_{trans} - S_1$ versus $W_x/(kT)$ is independent of mb^2: $S_{trans} - S_1$ always increases with decreasing W_x from zero at high W_x, but then when $W_x/(kT)$ approaches 1 (indicated by the dashed vertical line), it levels off rapidly. When $W_x/(kT)$ drops below 1, it remains essentially constant at the value for an ideal 2D monatomic gas of the same mass ($S_{trans} - S_1 = R \ln[(qe/\mathcal{A})/(M/\mathcal{A})] = R \ln[(qe/\mathcal{A})b^2] = R \ln[(2\pi mkTe/h^2)b^2]$, see above). As expected, this low-W_x limit increases by R ln 10 = 2.3 R and R ln 100 = 4.6 R, respectively, when mb^2 is increased by 10- and 100-fold, respectively.

Figure 6B compares the effect of barrier height on this same hindered translator entropy to that estimated by the 2D harmonic-oscillator (HO) approximation using the same frequency, ν_x, from eq 2 for both x and y modes, for ethane on Pt(111). When $W_x/(kT)$ exceeds 100, the HO approximation is almost the same as the true hindered translator entropy. When $W_x/(kT)$ is between 1 and 100, the HO approximation underestimates the hindered translator entropy but only by small amounts (<0.5 R, with a maximum difference of 0.46 R occurring when $W_x/(kT)$ = 10). When $W_x/(kT)$ drops far below 1, the HO approximation greatly overestimates the hindered translator entropy, which levels out as noted above. It is clear from Figure 6 that, to a good approximation, the translational contribution to the hindered translator entropy equals that given by the 2D HO approximation (to within 0.46 R) when $W_x/(kT) \geq 1$ and that for an ideal 2D monatomic gas (to within 0.12 R) when $W_x/(kT) < 1$. The cutoff between these two behaviors is surprisingly sharp. The locations and magnitudes of these maximum errors do not depend on mb^2 (not shown). It is also clear that the HO approximation severely overestimates the entropy of the hindered translator when kT exceeds the barrier. This was explained above, where the same effect was seen in Figure 4A.

Figure 7A shows how the rotational entropy for ethane on Pt(111) depends upon $W_r/(kT)$, the rotational barrier normalized to kT, where T = 106 K, the experimental T_{max} for ethane on Pt(111). This is the curve labeled "$I/n^2 \times 1$". This entropy is nearly constant when $W_r/(kT)$ is below 1 and then decreases with increasing $W_r/(kT)$ and asymptotically approaches zero for large $W_r/(kT)$. As shown above, the parameters I and n are always grouped together as I/n^2 in the equations that determine S for the hindered rotor. For a given value of $W_r/(kT)$, the rotational entropy also increases with I/n^2 (the adsorbate's reduced moment of inertia divided by the square of the number of energy barriers per rotation) as shown. The general shape of S_{rot} versus $W_r/(kT)$ is independent of I/n^2, and when $W_r/(kT)$ drops below 1 (indicated by the dashed vertical line) it becomes essentially constant at the value for a free 1D rotor of the same moment of inertia, which is given by $S_{rot} = R \ln[(qe)^{1/2}] = R \ln[((2\pi)^3(I/n^2)kTe/h^2)^{1/2}]$.[39] As expected, in this low-barrier limit, S_{rot} increases by R ln $10^{1/2}$ = 1.15 R and R ln $100^{1/2}$ = 2.30 R when I/n^2 is increased by 10- and 100-fold, respectively.

Figure 7B compares the effect of barrier height on this same hindered rotor entropy to that estimated with the HO approximation using the same frequency, ν_r from eq 15, for ethane on Pt(111). When $W_r/(kT)$ exceeds 100, the HO approximation is almost the same as the true hindered rotor entropy. When $W_r/(kT)$ is between 1 and 100, the HO approximation underestimates the hindered rotor entropy, but only by small amounts (<0.23 R). When $W_r/(kT)$ drops far below 1, the HO approximation greatly overestimates the hindered rotor entropy. It is clear from Figure 7B that, to a good approximation, the hindered rotor entropy equals that from the HO approximation (to within 0.23 R) when $W_r/(kT) \geq 1$ and equals that for a free 1D rotor entropy (within 0.06 R)

DOI: 10.1021/acs.jpcc.5b11616
J. Phys. Chem. C 2016, 120, 9719−9731

when $W_r/(kT) < 1$. Again, the cutoff between these two behaviors is surprisingly sharp. The locations and magnitudes of these maximum errors do not depend on I/n^2 (not shown). It is also clear that the HO approximation severely overestimates the entropy of the hindered rotor when kT exceeds the barrier. This was explained above, where the same effect was seen in Figure 4B.

Although the comparisons to experimental entropies in Figure 5 were done for small molecules adsorbed on the Pt(111) surface, this model is also expected to be applicable for molecular fragments and other molecules and for other surfaces, provided they have potential energy surfaces similar to Figure 1.

For practical calculations of surface reaction rates, one could assume that W_x is ~10% of the adsorption energy (see above). Based on this estimate, if W_x/kT is <0.4, it is probably safe to work with this estimate since it gives the entropy of the ideal 2D gas limit even if incorrect by a factor of 3. If $W_x/kT > 0.4$, W_x probably should be calculated more carefully, at least for transition states and adsorbed intermediates that have a significant degree of rate control. Similarly, one could assume that W_r is ~1% of the adsorption energy (see above). Based on this estimate, if W_r/kT is <0.4, it is probably safe to work with this estimate since it gives the entropy of a free rotor even if this barrier limit is incorrect by a factor of 3.

5. CONCLUSIONS

An easy to implement and accurate method to determine entropies of adsorbed molecules and molecular fragments was developed that models motions of the adsorbate parallel to the surface as two hindered translators and a hindered rotor. Our approach only requires the energy barrier heights for translations and rotation of the adsorbate for these modes, as well as the surface symmetry and nearest-neighbor site distance. The method is validated by proving that it has the proper high-temperature and low-temperature limits (i.e., the ideal 2D gas and ideal 2D lattice gas, respectively) and, for intermediate temperatures, by comparison of its predictions with experimental values for four adsorbed molecules on Pt(111). All barriers were calculated using DFT, both with and without vdW correction, and the frequencies were determined by fitting the DFT minima and maxima to a cosine wave. The entropies determined by this method using DFT with vdW corrections are in very good agreement with the experimental entropies.

The translational and rotational contributions to the entropy of a hindered translator/hindered rotor calculated with this new method are, in general, very closely approximated (to within <0.25 R error per mode) by the corresponding harmonic oscillator (i.e., lattice gas) entropy (calculated using ν_x and ν_r, respectively) when kT is less than the barrier. When kT exceeds the barrier, the hindered translator/hindered rotor model is closely approximated (to within 0.1 R) by the entropy of an ideal 2D monatomic gas of the same mass and a free 1D rotor with the same moment of inertia, respectively. There exists a very sharp cutoff between the temperature ranges of applicability of these simple two approximations (see Figures 6 and 7). The harmonic oscillator/lattice gas model severely overestimates the entropy when kT exceeds the barrier by much.

These calculated adsorbate entropies, combined with transition-state theory, can be used to calculate rate constants and prefactors for elementary reaction steps to build microkinetic models.

■ ASSOCIATED CONTENT

Supporting Information

The Supporting Information is available free of charge on the ACS Publications website at DOI: 10.1021/acs.jpcc.5b11616.

Binding energies and configurations of adsorbates on Pt(111) (PDF)

■ AUTHOR INFORMATION

Corresponding Author

*E-mail: liney.arnadottir@oregonstate.edu.

Notes

The authors declare no competing financial interest.

■ ACKNOWLEDGMENTS

Acknowledgment is made to the donors of the American Chemical Society Petroleum Research Fund for support of this research. We thank Lars Grabow, Jason Weaver, and Daniel Auerbach for very helpful discussions and careful reading of the manuscript.

■ REFERENCES

(1) Campbell, C. T.; Lytken, O. Experimental Measurements of the Energetics of Surface Reactions. *Surf. Sci.* **2009**, *603*, 1365−1372.

(2) Brown, W. A.; Kose, R.; King, D. A. Femtomole Adsorption Calorimetry on Single-Crystal Surfaces. *Chem. Rev.* **1998**, *98*, 797−831.

(3) Campbell, C. T.; Sellers, J. R. V. The Entropies of Adsorbed Molecules. *J. Am. Chem. Soc.* **2012**, *134*, 18109−18115.

(4) Hill, T. L. *An Introduction to Statistical Thermodynamics*; Addison-Wesley: Reading, MA, 1960.

(5) Dumesic, J. A.; Huber, G. W.; Boudart, M. Microkinetics. In *Handbook of Heterogeneous Catalysis*, 2nd ed.; Ertl, G., K, H., Schüth, F., Weitkamp, J., Ed.; Wiley-VCH Verlag Gmbh: Weinheim, Germany, 2008; pp 1445−1462.

(6) Reuter, K.; Frenkel, D.; Scheffler, M. The Steady State of Heterogeneous Catalysis, Studied by First-Principles Statistical Mechanics. *Phys. Rev. Lett.* **2004**, DOI: 10.1103/PhysRevLett.93.116105.

(7) Gokhale, A. A.; Kandoi, S.; Greeley, J. P.; Mavrikakis, M.; Dumesic, J. A. Molecular-Level Descriptions of Surface Chemistry in Kinetic Models Using Density Functional Theory. *Chem. Eng. Sci.* **2004**, *59*, 4679−4691.

(8) Honkala, K.; Hellman, A.; Remediakis, I. N.; Logadottir, A.; Carlsson, A.; Dahl, S.; Christensen, C. H.; Norskov, J. K. Ammonia Synthesis from First-Principles Calculations. *Science* **2005**, *307*, 555−558.

(9) Reuter, K.; Scheffler, M. First-Principles Kinetic Monte Carlo Simulations for Heterogeneous Catalysis: Application to the CO Oxidation at RuO2(110). *Phys. Rev. B: Condens. Matter Mater. Phys.* **2006**, *73*, 045433.

(10) Gokhale, A. A.; Dumesic, J. A.; Mavrikakis, M. On the Mechanism of Low-Temperature Water Gas Shift Reaction on Copper. *J. Am. Chem. Soc.* **2008**, *130*, 1402−1414.

(11) Pitzer, K. S.; Gwinn, W. D. Energy Levels and Thermodynamic Functions for Molecules with Internal Rotation I. Rigid Frame with Attached Tops. *J. Chem. Phys.* **1942**, *10*, 428−440.

(12) McClurg, R. B.; Flagan, R. C.; Goddard, W. A. The Hindered Rotor Density-of-States Interpolation Function. *J. Chem. Phys.* **1997**, *106*, 6675−6680.

(13) Henkelman, G.; Uberuaga, B. P.; Jonsson, H. A Climbing Image Nudged Elastic Band Method for Finding Saddle Points and Minimum Energy Paths. *J. Chem. Phys.* **2000**, *113*, 9901−9904.

(14) Henkelman, G.; Jonsson, H. Improved Tangent Estimate in the Nudged Elastic Band Method for Finding Minimum Energy Paths and Saddle Points. *J. Chem. Phys.* **2000**, *113*, 9978−9985.

DOI: 10.1021/acs.jpcc.5b11616
J. Phys. Chem. C 2016, 120, 9719−9731

(15) Jónsson, H.; Mills, G.; Jacobsen, K. W. *Classical and Quantum Dynamics in Condensed Phase Simulations*; World Scientific: Singapore, 1998; p 385.
(16) Payne, S. H.; McEwen, J. S.; Kreuzer, H. J.; Menzel, D. Lateral Interactions and Nonequilibrium in Adsorption and Desorption. Part 2. A Kinetic Lattice Gas Model for (2 × 2)-(3O+NO)/Ru(001). *Surf. Sci.* **2006**, *600*, 4660−4669.
(17) Kreuzer, H. J. Thermal-Desorption Kinetics. *Langmuir* **1992**, *8*, 774−781.
(18) Payne, S. H.; McEwen, J. S.; Kreuzer, H. J.; Menzel, D. Adsorption and Desorption of CO on Ru(0001): A Comprehensive Analysis. *Surf. Sci.* **2005**, *594*, 240−262.
(19) Peterson, L. D.; Kevan, S. D. Lattice-Gas Virial-Coefficients from Isothermal Desorption Measurements - Co on Cu(001) and Cu(011). *Phys. Rev. Lett.* **1990**, *65*, 2563−2566.
(20) Wu, K. J.; Kevan, S. D. Isothermal Coverage Dependent Measurements of NH3 and ND3 Desorption from Cu(001). *J. Chem. Phys.* **1991**, *95*, 5355−5363.
(21) Campbell, C. T.; Sprowl, L. H.; Árnadóttir, L. Calculating Equilibrium and Rate Constants for Adsorbates: 2D Ideal Gas, 2D Ideal Lattice Gas, and Hindered Translator Models. *J. Phys. Chem.*, submitted.
(22) Donaldson, D. J.; Ammann, M.; Bartels-Rausch, T.; Poeschl, U. Standard States and Thermochemical Kinetics in Heterogeneous Atmospheric Chemistry. *J. Phys. Chem. A* **2012**, *116*, 6312−6316.
(23) McQuarrie, D. A. *Statistical Mechanics*; University Science Books: Sausalito, 2000; pp 68−157.
(24) Kresse, G.; Hafner, J. Ab Initio Molecular Dynamics for Liquid Metals. *Phys. Rev. B: Condens. Matter Mater. Phys.* **1993**, *47*, 558−561.
(25) Kresse, G.; Hafner, J. Ab Initio Molecular-Dynamics Simulation of the Liquid-Metal-Amorphous-Semiconductor Transition in Germanium. *Phys. Rev. B: Condens. Matter Mater. Phys.* **1994**, *49*, 14251−14269.
(26) Kresse, G.; Furthmuller, J. Efficiency of Ab-Initio Total Energy Calculations for Metals and Semiconductors Using a Plane-Wave Basis Set. *Comput. Mater. Sci.* **1996**, *6*, 15−50.
(27) Kresse, G.; Furthmuller, J. Efficient Iterative Schemes for Ab Initio Total-Energy Calculations Using a Plane-Wave Basis Set. *Phys. Rev. B: Condens. Matter Mater. Phys.* **1996**, *54*, 11169−11186.
(28) Kresse, G.; Joubert, D. From Ultrasoft Pseudopotentials to the Projector Augmented-Wave Method. *Phys. Rev. B: Condens. Matter Mater. Phys.* **1999**, *59*, 1758−1775.
(29) Blochl, P. E. Projector Augmented-Wave Method. *Phys. Rev. B: Condens. Matter Mater. Phys.* **1994**, *50*, 17953−17979.
(30) Perdew, J. P.; Burke, K.; Ernzerhof, M. Generalized Gradient Approximation Made Simple. *Phys. Rev. Lett.* **1996**, *77*, 3865−3868.
(31) Perdew, J. P.; Burke, K.; Ernzerhof, M. Generalized Gradient Approximation Made Simple (vol 77, pg 3865, 1996). *Phys. Rev. Lett.* **1997**, *78*, 1396−1396. http://journals.aps.org/prl/abstract/10.1103/PhysRevLett.78.1396.10.1103/PhysRevLett.78.1396
(32) Grimme, S.; Antony, J.; Ehrlich, S.; Krieg, H. A Consistent and Accurate Ab Initio Parametrization of Density Functional Dispersion Correction (DFT-D) for the 94 Elements H-Pu. *J. Chem. Phys.* **2010**, *132*, 154104.
(33) Monkhorst, H. J.; Pack, J. D. Special Points for Brillouin-Zone Integrations. *Physics Review B* **1976**, *13*, 5188−5192.
(34) Ashcroft, N. W.; Mermin, N. D. *Solid State Physics*; Holt, Rinehart and Winston: N. Y., 1976.
(35) Bahn, S. R.; Jacobsen, K. W. An Object-Oriented Scripting Interface to a Legacy Electronic Structure Code. *Comput. Sci. Eng.* **2002**, *4*, 56−66.
(36) Medford, A. J.; Shi, C.; Hoffmann, M. J.; Lausche, A. C.; Fitzgibbon, S. R.; Bligaard, T.; Norskov, J. K. CatMAP: A Software Package for Descriptor-Based Microkinetic Mapping of Catalytic Trends. *Catal. Lett.* **2015**, *145*, 794−807.
(37) Campbell, C. T.; Árnadóttir, L.; Sellers, J. R. V. Kinetic Prefactors of Reactions on Solid Surfaces. *Z. Phys. Chem.* **2013**, *227*, 1435−1454.
(38) Piccini, G.; Alessio, M.; Sauer, J.; Zhi, Y.; Liu, Y.; Kolvenbach, R.; Jentys, A.; Lercher, J. A. Accurate Adsorption Thermodynamics of Small Alkanes in Zeolites. Ab Initio Theory and Experiment for H-Chabazite. *J. Phys. Chem. C* **2015**, *119*, 6128−6137.
(39) Truhlar, D. G. A Simple Approximation for the Vibrational Partition-Function of a Hindered Internal-Rotation. *J. Comput. Chem.* **1991**, *12*, 266−270.

DOI: 10.1021/acs.jpcc.5b11616
J. Phys. Chem. C 2016, 120, 9719−9731